TECHNICAL ARTICLE

Effect of cryogenic milling on Al7075 prepared by spark plasma sintering method

Frantisek Lukac,[1,a] Tomas Chraska,[1] Orsolya Molnarova,[2] Premysl Malek,[2] and Jakub Cinert[1,3]
[1]*Institute of Plasma Physics, Academy of Sciences of the Czech Republic, Czech Republic*
[2]*Department of Physics of Materials, Mathematics and Physics Faculty, Charles University, Czech Republic*
[3]*Department of Electrotechnology, Faculty of Electrical Engineering, Czech Technical University, Czech Republic*

(Received 16 October 2016; accepted 26 March 2017)

Precipitation of secondary intermetallic phases in aluminium alloy Al7075 sintered by spark plasma sintering method from powders milled at room and cryogenic temperature was studied by X-ray powder diffraction. Deformation energy stored during cryogenic milling influences the precipitation in Al7075 alloy. High temperature X-ray diffraction experiment revealed the potential for further precipitation strengthening of samples prepared by spark plasma sintering of milled powders. It was established that the correction of absorption edge of metal $K\beta$-line filter used for laboratory sources greatly enhances the precision of quantitative Rietveld analysis as well as the determination of precipitates' crystallite sizes. © *2017 International Centre for Diffraction Data*.
[doi:10.1017/S0885715617000483]

Key words: Intermetallic precipitates, cryogenic milling, powder metallurgy, ultrafine-grained materials, Al7075

I. INTRODUCTION

Powder metallurgy is a perspective method for processing of metallic materials, which exhibit excellent properties not achievable in cast metal ingots. Powders are usually prepared either by milling of bulk alloy material to chosen granularity or by using rapid solidification techniques e.g. gas atomization. Further milling of these original powders introduces high deformation energy into the material, which can serve as an energy reservoir for recrystallization during the following compaction step. Consequently, fine-grained microstructure with attractive properties can be formed. Metallic powders prepared by high energy milling contain increased amount of alloying elements in solid solution because of a high degree of disorder and high density of crystal lattice defects. The presence of intermetallic precipitates is limited to nanoscale sizes only (Molnarova *et al.*, 2015). In order to increase the intensity of milling process by embrittlement of rather ductile metals, the cryogenic milling was introduced.

Powder compaction method has emerged as a limiting factor for achieving bulk materials, which would maintain all benefits achieved by milling. Spark plasma sintering (SPS) technique, which combines simultaneous heating by DC current pulses with application of uniaxial pressure, provides an exceptional advantage of fast heating/cooling rates when compared with conventional sintering methods (Guillon *et al.*, 2014). The short exposition of materials to high temperature during SPS helps to suppress the undesired grain growth and changes in phase composition.

The commercial Al7075 is a typical precipitation strengthened material. Its high strength results from the precipitation sequence occurring either at room temperature (RT) (natural ageing) or at elevated temperatures (artificial ageing) after solution treatment. The well-known sequence in this type of alloys—supersaturated solid solution—Guinier Preston zones – metastable η' phase—stable η-$MgZn_2$ phase (Liu *et al.*, 2010) can be modified by variations in chemical composition, presence of microstructure defects or by occurrence of further sites for heterogeneous nucleation. Consequently, other complex phases can be formed.

II. EXPERIMENTAL

Samples of the Al7075 aluminium alloy with the alloying elements content (in wt%) of 6.2% Zn, 2.7% Mg, 1.7% Cu and 0.1% Fe were produced by gas atomization with nitrogen by Nanoval GmbH & Co. KG, Berlin. Atomized powder was subsequently milled in high energy ball mill UNION HD01 Lab Attritor either at RT in Ar gas or in cryogenic regime in liquid nitrogen. The powders were consolidated by pulsed electric current sintering machine SPS 10-4 Thermal Technology, USA, under following sintering conditions: sintering temperature 425 °C, pressure of 80 MPa, vacuum of 10 Pa and sintering time of 4 min. Virtually no porosity was found in the samples sintered at these conditions (Becker *et al.*, 2015). Sintering was performed in graphite moulds and graphite foils, which were subsequently ground away and the surface of samples was then polished up to the 1 μm of abrasive particles size.

Phase compositions and lattice parameters were determined from X-ray diffraction (XRD) patterns obtained at RT by Cu$K\alpha$ radiation (40 kV, 40 mA; constant volume mode; 2θ range from 15° to 90° with 0.02° step and 384 s time per step) and 1D LynxEye detector (Ni β filter in front of the detector) mounted on D8 Discover (Bruker AXS, Germany)

[a]Author to whom correspondence should be addressed. Electronic mail: lukac@ipp.cas.cz

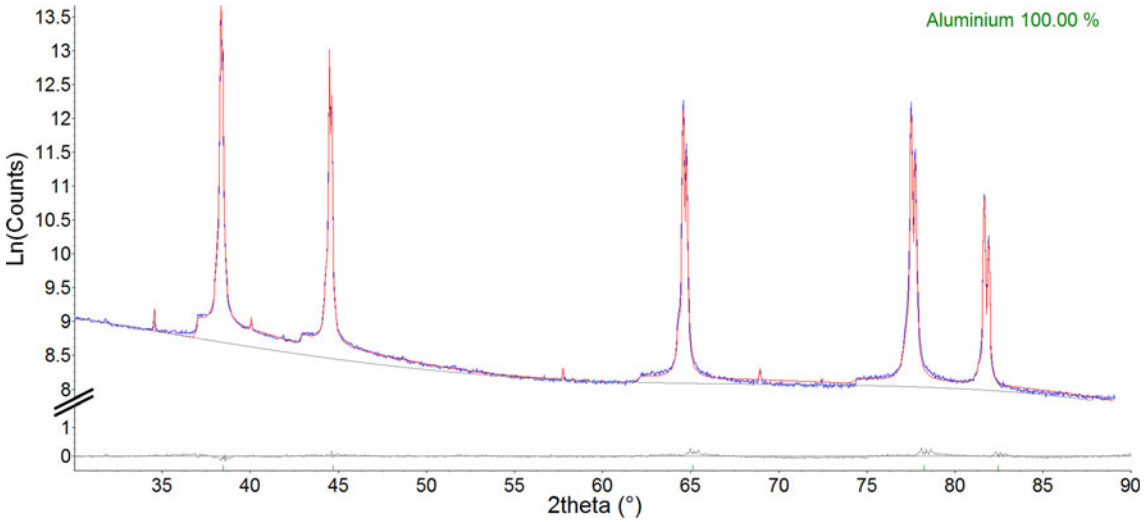

Figure 1. (Colour online) Rietveld refinement for pure Al powder with absorption edge and tube tails corrections. $R_{wp} = 7.1\%$.

and subsequent Rietveld refinement performed in TOPAS V5 (Coelho, 2016). Fundamental Parameters Approach was used for calculation of profile broadening because of instrumental effects.

High temperature XRD experiments were performed in modular temperature chamber with TC-basic (mri, DE) in vacuum up to 10^{-6} mbar by Cu$K\alpha$ (40 kV, 40 mA; constant volume mode; 2θ range from 33° to 54° with 0.03° step and 768 s time per step). Sample was mounted on Pt-Rh heater plate directly connected to thermocouple under the sample. Sample was held on the set temperature for 5 min before data collection.

Sizes of coherently diffracting domains (CDD) of the secondary phase were determined from broadening of Lorentzian component of pseudo-Voigt function and calculated as volume weighted average derived from full width at half maximum (Scardi *et al.*, 2004).

III. RESULTS AND DISCUSSION

The advent of position sensitive detectors dedicated for the laboratory diffractometers gave rise to the high intensity data obtained in relatively short measuring times. On the other hand, high intensity gives rise to several features of the laboratory sources. In particular, because of the employment of metal $K\beta$-line filters, absorption edge influences the diffraction pattern and complicates accurate fitting of the low-energy peaks tail regions.

TOPAS version 5 offers the functionality of emission profile correction for an absorption edge of $K\beta$-line filter. It employs five fitting parameters of the step function simulating the absorption edge of Ni metal filter inserted into the secondary beam path. This approach greatly enhances the sensitivity of quantitative Rietveld analysis, see Figure 1. Strong reflections in measured precipitation-strengthened alloys usually come from the aluminium-rich matrix. The lower-angle area in the vicinity of a strong reflection starting from the absorption edge up to the maximum intensity can be misinterpreted as another broad peak. Moreover, the higher-angle tail is a distinct feature of the diffraction pattern, which is also realistically resolved within this approach up to a chosen maximum wavelength of Bremsstrahlung, we used $\lambda_{max} = 2.7$ Å. Therefore, broad reflections of nanocrystalline secondary phases are no longer artificially broadened by the absence of correct background fit in this range and the whole fit is generally fitted significantly better.

To Cu$K\alpha$ emission profile consisting of five lines (Berger, 1986) was added one line representing the Cu$K\beta$ remnants unfiltered by Ni filter with the wavelength of 1.39 222 Å (Hölzer *et al.*, 1997). In addition, the so-called "tube tails"

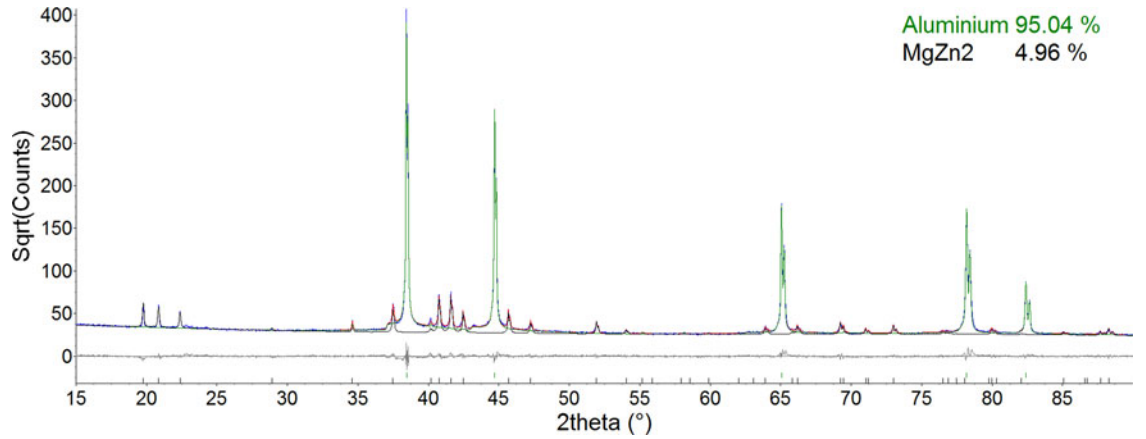

Figure 2. (Colour online) Rietveld refinement of XRD pattern for SPS sample from powder after cryogenic milling at 400 RPM for 3 h. $R_{wp} = 5.9\%$.

https://doi.org/10.1017/S0885715617000483 Published online by Cambridge University Press

TABLE I. Results of Rietveld refinement for SPS samples from atomised and milled Al7075 powders: weight fraction of identified phases and coherently diffracting domains size for $MgZn_2$ phase.

Preparation of powder	Aluminium (wt%)	$MgZn_2$ (wt%)	Al_2CuMg (wt%)	CDD $MgZn_2$ (nm)
Gas atomisation	95.1(2)	4.03(7)	0.9(2)	63(2)
Cryogenic 180 RPM/3 h	95.31(9)	4.05(5)	0.64(8)	95(3)
Cryogenic 400 RPM/3 h	95.04(4)	4.96(4)		127(3)
RT 180 RPM/3 h	97.41(4)	2.59(4)		74(3)
RT 400 RPM/3 h	95.3(1)	4.11(5)	0.6(1)	110(3)
RT 400 RPM/8 h	95.19(5)	4.81(5)		130(4)

The errors of the fit parameters are displayed in parentheses for the last digit.

corrections were also included in the fit as described in (Bergmann *et al.*, 2000). Figure 1 shows the diffraction data collected on a pure aluminium powder in order to determine the absorption edge correction parameters, which were used as initial values of fitting parameters for fits performed on Al7075 alloy samples.

Figure 2 shows diffraction data of atomized powders in logscale and demonstrates how sensitive the result of the fit is to the corrections of the tails when $MgZn_2$ phase precipitates are present. Typically the R_{wp} value without these corrections is by 50% higher when compared to the case with the absorption edge and tube tails corrections included. Moreover, owing to the absence of tails between (111) and (002) Al reflections the fraction of secondary precipitates is artificially enhanced. The effect is even more evident if the crystallite sizes are in low nanometer range and broad profiles are embedded into incorrect background.

Results of quantitative Rietveld refinement in samples spark plasma sintered from nanocrystalline powders after gas atomisation and milling are summarized in Table I; please note that the given errors are derived purely from mathematical calculations (Madsen *et al.*, 2012). Besides minor hexagonal phase isomorphous with $MgZn_2$ phase (Wert, 1981), the Al_2CuMg orthorhombic phase was present in SPS sample from atomized Al7075 powder. This phase also appeared in SPS samples after cryogenic milling at 180 RPM (revolutions per minute) for 3 h and RT milling at 400 RPM for 3 h. Highest $MgZn_2$ content was present after cryogenic milling at 400 RPM for 3 h. This confirms that more deformation energy is stored in the material during longer and more intense milling process. This energy is subsequently consumed during sintering for nucleation and coalescence of precipitates and for acceleration of further precipitation growth.

High temperature XRD experiment was performed on the SPS sample sintered from powder prepared by cryogenic milling at 400 RPM for 3 h. Figure 3 shows the influence of temperature on the weight fraction of $MgZn_2$ precipitates and on the size of coherently diffracting domains. An abrupt increase in fraction of $MgZn_2$ phase started at 250 °C and was accompanied by a decrease of coherently diffracting domain size. This indicates precipitation of new crystallites of $MgZn_2$ from the matrix, which means that during the SPS process the precipitation of $MgZn_2$ was not completed because of the fast cooling rate. Therefore, samples prepared by SPS possess the potential of further strengthening by new precipitation achievable by tailored heat treatment. Furthermore, the growth of CDD size took place at the temperature of 400 °C, which was associated by the growth of precipitates. After this temperature cycle the final CDD size was smaller than the initial one after SPS.

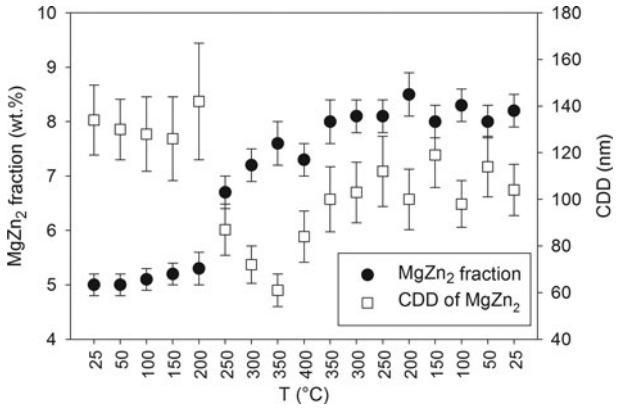

Figure 3. Fraction of $MgZn_2$ precipitates and its coherently diffracting domains during HT XRD experiment in SPS sample sintered from powder prepared by cryogenic milling at 400 RPM for 3 h.

IV. CONCLUSIONS

The correction for $K\beta$-filter absorption edge in powder XRD data with intense reflection greatly enhances the quantitative Rietveld refinement especially when crystallites of minor phases are very small. Moreover, coherently diffracting domains of precipitates with content of few weight percent can be fitted more confidently, which allows optimization of precipitation sequences and heat treatment of alloys by XRD method. Spark plasma sintered compacts from milled powders have potential for further precipitation hardening. Cryogenic milling introduces higher deformation energy into powders and supports precipitation of secondary phases in SPS compact samples.

ACKNOWLEDGEMENTS

This work was financially supported by the grant GACR 15-15609S. Authors are grateful to Dr Zdenek Pala for valuable consultations. One author, Orsolya Molnarova, is grateful for financial support from the grant SVV-2016-260213.

Becker, H., Dopita, M., Stráská, J., Málek, P., Vilémová, M., and Rafaja, D. (**2015**). "Microstructure and properties of spark plasma sintered Al–Zn–Mg–Cu alloy," Acta Phys. Polon. A **128**(4), 602–605. Doi: 10.12693/APhysPolA.128.602.

Berger, H. (**1986**). "Study of the Kα emission spectrum of copper," X-Ray Spectrom. **15**(4), 241–243. Doi: 10.1002/xrs.1300150405.

Bergmann, J., Kleeberg, R., Haase, A., and Breidenstein, B. (**2000**). "Advanced fundamental parameters model for improved profile analysis," Mater. Sci. Forum 347–349, 303–308. Doi: 10.4028/www.scientific.net/MSF.347-349.303.

https://doi.org/10.1017/S0885715617000483 Published online by Cambridge University Press

Coelho, A. A. (**2016**). *TOPAS version 5 (Computer Software)* (Coelho Software, Brisbane).

Guillon, O., Gonzalez-Julian, J., Dargatz, B., Kessel, T., Schierning, G., Räthel, J., and Herrmann, M. (**2014**). "Field-assisted sintering technology/spark plasma sintering: mechanisms, materials, and technology developments: FAST/SPS: mechanisms, materials, and technology developments," Adv. Eng. Mater. **16**(7), 830–849. Doi: 10.1002/adem.201300409.

Hölzer, G., Fritsch, M., Deutsch, M., Härtwig, J., and Förster, E. (**1997**). "Kα1, 2 and Kβ1, 3 X-ray emission lines of the 3D transition metals," Phys. Rev. A **56**(6), 4554–4568. Doi: 10.1103/PhysRevA.56.4554.

Liu, J. Z., Chen, J. H., Yang, X. B., Ren, S., Wu, C. L., Xu, H. Y., and Zou, J. (**2010**). "Revisiting the precipitation sequence in Al–Zn–Mg-Based alloys by high-resolution transmission electron microscopy," Scr. Mater. **63**(11), 1061–1064. Doi: 10.1016/j.scriptamat.2010.08.001.

Madsen, I. C., Scarlett, N. V. Y., and Webster, N. A. S. (**2012**). "Quantitative phase analysis," In *Uniting Electron Crystallography and Powder Diffraction*, edited by U. Kolb, K. Shankland, L. Meshi, A. Avilov, and W. I. F. David (Springer Netherlands, Dordrecht), pp. 207–218. http://www.springerlink.com/index/10.1007/978-94-007-5580-2_19.

Molnarova, O., Malek, P., and Becker, H. (**2015**). "The investigation of the Al7075+1 wt% Zr alloy prepared using spark plasma sintering technology," *Metal* 2015: 24*th Int. Conf. Metallurgy and Materials*, 1221–1226.

Scardi, P., Leoni, M., and Delhez, R. (**2004**). "Line broadening analysis using integral breadth methods: a critical review," J. Appl. Crystallogr. **37**(3), 381–390. Doi: 10.1107/S0021889804004583.

Wert, J. A. (**1981**). "Identification of precipitates in 7075 Al after high-temperature aging," Scr. Metall. **15**(4), 445–447. Doi: 10.1016/0036-9748(81)90228-3.